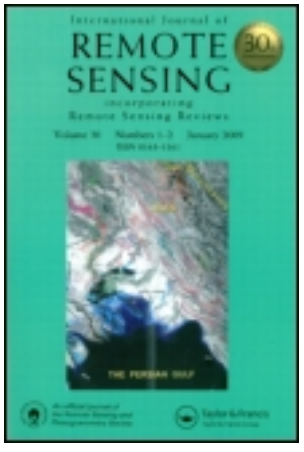

International Journal of Remote Sensing

Publication details, including instructions for authors and subscription information:
http://www.tandfonline.com/loi/tres20

Segmentation of multispectral high-resolution satellite imagery based on integrated feature distributions

Aiping Wang [a], Shugen Wang [b] & A. Lucieer [c]

[a] School of Geo-engineering and Surveying, Chang'an University, 126 Yanta Road, Xi'an, 710054, PR China

[b] School of Remote Sensing Information Engineering, Wuhan University, 129 Luoyu Road, Wuhan, 430079, PR China

[c] School of Geography and Environmental Studies, University of Tasmania, Hobart, Tasmania, 7001, Australia

Version of record first published: 30 Mar 2010.

To cite this article: Aiping Wang , Shugen Wang & A. Lucieer (2010): Segmentation of multispectral high-resolution satellite imagery based on integrated feature distributions, International Journal of Remote Sensing, 31:6, 1471-1483

To link to this article: http://dx.doi.org/10.1080/01431160903475308

International Journal of Remote Sensing
Vol. 31, No. 6, 20 March 2010, 1471–1483

Taylor & Francis
Taylor & Francis Group

Segmentation of multispectral high-resolution satellite imagery based on integrated feature distributions

AIPING WANG*†, SHUGEN WANG‡ and A. LUCIEER§
†School of Geo-engineering and Surveying, Chang'an University, 126 Yanta Road, Xi'an 710054, PR China
‡School of Remote Sensing Information Engineering, Wuhan University, 129 Luoyu Road, Wuhan 430079, PR China
§School of Geography and Environmental Studies, University of Tasmania, Hobart, Tasmania 7001, Australia

Texture features are useful for segmentation of high-resolution satellite imagery. This paper presents an efficient feature extraction method that considers the spatial and cross-band relationships of pixels in multispectral or colour images. The texture feature of an image region is represented by the joint distribution of two texture measures calculated from the first two principal components (PCs). Similarly, the spectral feature of the region is the joint distribution of greyscale pixel values of the two PCs. The texture distributions computed by a rotation invariant form of local binary patterns (LBP) and spectral distributions are adaptively combined into coarse-to-fine segmentation based on integrated multiple features (SIMF). The feasibility and effectiveness of the SIMF segmentation approach is evaluated with multispectral high-resolution satellite imagery and colour textured mosaic images under different conditions.

1. Introduction

High-resolution (H-res) satellite images have become commercially available and these images are increasingly used in various aspects of environmental monitoring and management. The fine resolution satellite imagery makes it possible to map land cover/use type in great spatial detail. On the other hand, the detail provided by the imagery brings challenges to the traditional pixel-based image analysis methods which often produce many 'salt and pepper' effects as the H-res satellite sensors increase the within-field spectral heterogeneity. Object-based image analysis (OBIA) techniques that make inferences based on spectral properties as well as other information such as object shape, texture, spatial relationships and human knowledge have shown to be useful for classifying H-res imagery (Hay and Castilla 2006). Segmentation is considered a crucial step in the OBIA approach.

Segmentation is the process of partitioning an image into several constituent components that have similar characteristics. In the field of computer vision, image segmentation is an important part of practically any automated image recognition system. Hundreds of image segmentation methods have been widely discussed in the last several decades, but not all of them are suitable for segmentation of satellite images. In remote sensing, many pixel-based classification methods, supervised or unsupervised, have been explored in the last three decades. The limitations of these

*Corresponding author. Email: wap531@163.com

International Journal of Remote Sensing
ISSN 0143-1161 print/ISSN 1366-5901 online
http://www.tandf.co.uk/journals
DOI: 10.1080/01431160903475308

pixel-based techniques are that pixels are not true geographical objects, that pixel topology is limited, and that pixel-based techniques largely neglect the spatial photo interpretive elements (e.g. texture, context, shape). In addition, increased variability implicit within H-res imagery confuses traditional pixel-based classifiers, which results in lower classification accuracies (Hay and Castilla 2006).

Segmentation of H-res satellite imagery has recently drawn considerable attention. Several new segmentation algorithms have been examined by a number of researchers. The fractal net evolution approach (FNEA) embedded in the commercial software eCognition was thoroughly described by Baatz and Schäpe (2000). Various research projects have demonstrated the potential of this multiscale segmentation approach (Hay *et al.* 2003), yet it still suffers from some limitations, e.g. it cannot be fully exploited because of the lack of a theoretical framework and users have to find useful segmentation levels by 'trial and error' (Hay *et al.* 2003). Pesaresi and Benediktsson (2001) proposed a new morphological multiscale segmentation algorithm based on the morphological characteristic of connected components in images which is particularly well suited for complex image scenes such as city scenes of aerial or H-res satellite images. Examples of more recent algorithms include the floating point-based watershed transform and then size-constrained region merging (Chen *et al.* 2004, Chen *et al.* 2006), multiscale object-specific segmentation (MOSS) (Hay *et al.* 2005), segmentation based on the Gaussian hidden Markov random field model (Gigandet *et al.* 2005) and automatic segmentation of H-res satellite imagery by integrating texture, intensity and colour features (Hu *et al.* 2005).

There has been limited research on segmentation based on integrated multiple features (SIMF) (Chen and Chen 2002, Hu *et al.* 2005). Chen and Chen (2002) evaluated a colour texture segmentation approach combining colour and local edge patterns by constant weights; however, the method only performs well on some simple colour texture images and natural scenes and it is not suitable for complex H-res satellite images. The approach presented by Hu *et al.* (2005) performs relatively well on H-res satellite imagery but the weights of three features are difficult to determine. Moreover, few experimental studies have thoroughly evaluated SIMF algorithms.

The choice of highly discriminating features (Ojala and Pietikäinen 1999) and how to combine the features are the most important factors for SIMF. In this study, we present a region-based unsupervised segmentation method, which uses features integrating texture and spectral distributions. Unlike existing feature extraction methods, our method considers the cross-band relationships between image pixels. We combine the texture and spectral features to measure the similarity of adjacent image regions during the multiscale segmentation process following Chen and Chen (2002), Hu *et al.* (2005), and Ojala and Pietikäinen (1999). The main objective of this study is to apply and evaluate the new feature extraction method and its ability in segmentation of H-res satellite images. A further objective is to explore the factors of SIMF that affect the segmentation results through comparative experimental investigations.

The paper is organized as follows. §2 explains the feature extraction method. The segmentation methodology is presented in §3. In §4, we carry out several experiments and present the segmentation results. §5 concludes the paper with discussion and conclusion.

2. Feature description

In the whole segmentation process, the features of an image region are computed by a novel texture and spectral feature extraction method which considers the cross-band relationships. Principal component analysis (PCA) is adopted to remove redundant

information and make it convenient to extract features of multispectral images. More specifically, we obtain the first two principal components (PCs) of multispectral (i.e. blue, green, red and near-infrared) H-res imagery through PCA. These first two PCs collect most of the information of the H-res imagery. Then the texture and spectral features are calculated from the two PCs which are denoted by discrete two-dimensional histograms. Their two dimensions correspond to the two PC variables respectively.

2.1 *LBP texture operator*

The texture operator of local binary patterns (LBP) was first proposed as a complementary measure of local image contrast by Ojala *et al.* (1996) and was extended by subsequent studies. Due to its major advantages of computational simplicity and robustness to rotation and monotonic transformation of greyscale, it has been frequently used in many studies, such as texture segmentation or classification (Chen and Chen 2002, Ojala *et al.* 2006), moving objects detection (Heikkila and Pietikäinen 2006) and segmentation of remote sensing imagery (Hu *et al.* 2005, Lucieer *et al.* 2005).

The name 'local binary patterns' reflects the functionality of the operator, i.e. a local neighbourhood is thresholded at the grey value of the centre pixel into a binary pattern (Ojala *et al.* 2002). The original LBP was produced by multiplying the thresholded values with weights given to the corresponding pixels and summing the results (Mäenpää 2003) (see figure 1). Ojala *et al.* (2002) proposed a greyscale invariant LBP form $L_{P,R}$, which is defined as:

$$L_{P,R} = \sum_{p=0}^{P-1} 2^p s_p, \tag{1}$$

where

$$s_p = s(g_p - g_c) = \begin{cases} 0, g_p < g_c \\ 1, g_p \geq g_c \end{cases}, \tag{2}$$

where P is the number of neighbouring pixels on a circle of radius R, g_c corresponds to the grey value of the centre pixel of a texture unit and g_p is the grey value of its neighbourhood (see figure 2).

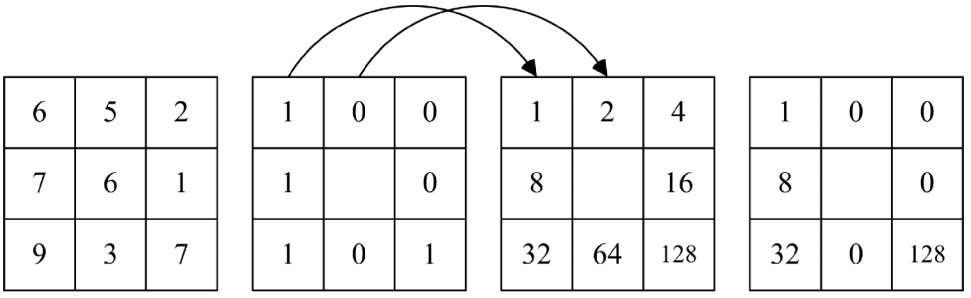

Figure 1. Calculation of the original LBP.

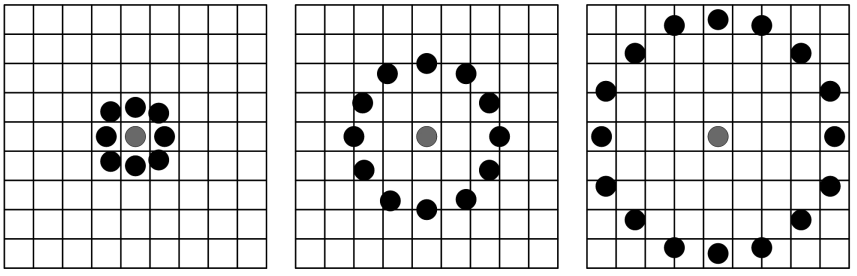

Figure 2. Circularly symmetric neighbour sets for different P and R. Samples that do not exactly match the pixel grid are obtained via interpolation.

In order to achieve rotation invariance, Ojala *et al.* (2002) presented the term of 'Uniform', whose measure corresponds to the number of spatial transitions (bitwise 0/1 changes) in the binary patterns. The LBP operator based on 'Uniform' patterns, $L_{P,R}^{riu2}$, can be defined as:

$$L_{P,R}^{riu2} = \begin{cases} \sum_{p=0}^{P-1} s(g_p - g_c), & if \quad U(L_{P,R}) \le 2 \\ P+1, & otherwise \end{cases}, \tag{3}$$

where

$$U(L_{P,R}) = \left|s(g_{p-1} - g_c) - s(g_0 - g_c)\right| + \sum_{p=1}^{P-1} \left|s(g_p - g_c) - s(g_{p-1} - g_c)\right|. \tag{4}$$

However, $L_{P,R}^{riu2}$ is defined in the case of regular textures, e.g. Brodatz's textures which consist of the vast majority of 'Uniform' patterns. It is not the case of satellite imagery according to our experiments. So we present a rotation invariant LBP form $L_{P,R}^{ri}$ that is more suitable for satellite images:

$$L_{P,R}^{ri} = \frac{1}{P}\sum_{i=0}^{P-1} \left\{R_L(L_{P,R}, i) | i = 0, 1, \cdots, P-1\right\}, \tag{5}$$

where R_L is defined as:

$$R_L(L_{P,R}, i) = \begin{cases} \sum_{p=i}^{P-1} 2^{p-i} s_p + \sum_{p=0}^{i-1} 2^{P-i+p} s_p, & i > 0 \\ L_{P,R}, & i = 0 \end{cases}, \tag{6}$$

2.2 *Texture and spectral distributions*

Most studies using texture features only use grey-level or single band images. This approach does not take into account the cross-band relationships of multispectral pixels (Hu *et al.* 2005). Lucieer *et al.* (2005) considered the cross-band relationships by multivariate texture model which, however, is too complicated for images of more than three bands. In this study, the texture feature of an image region is evaluated by the joint distribution, i.e. a discrete two-dimensional histogram, of two LBP texture images derived from the first two PCs of the image region. In the following

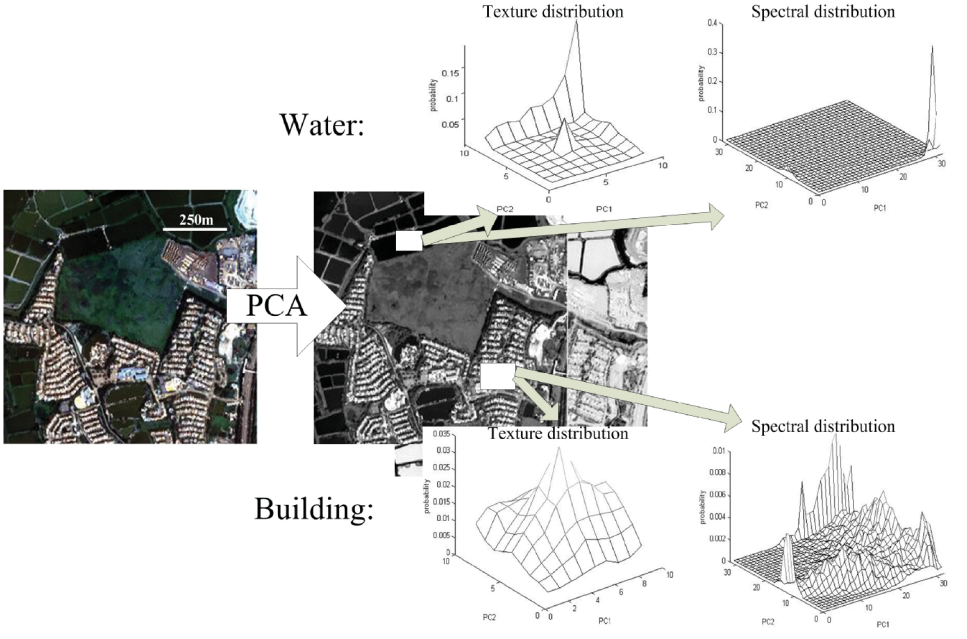

Figure 3. The texture and spectral distributions of different objects in a multispectral IKONOS image.

experiments, we apply several LBP forms at a range of neighbourhood scales, i.e. $L_{8,1}$, $L^{riu2}_{8,1}$, $L^{riu2}_{24,3}$ and $L^{ri}_{8,1}$, to calculate the texture distribution L_{pc1}/L_{pc2} of an image region and compare their effectiveness in multispectral image segmentation.

The spectral feature of an image region is the joint distributions of grey values of its first two PCs. The features have good discrimination ability as shown in figure 3. As the number of bins used in the quantization of the feature space is a trade-off between the discriminative power and the stability of the feature transform, we set the bins of spectral distribution as 32 by 32.

2.3 *Similarity measure*

Several possible similarity measures have been proposed for histograms, such as histogram intersection, log-likelihood statistic or G-statistic and chi-square statistic (χ^2).We chose a non-parametric statistic, the G-statistic, as a pseudo-metric for measuring the similarity of feature distributions between two regions, following Ojala and Pietikäinen (1999). The similarity between sample and model histograms is computed by the formula:

$$G = 2\left(\left[\sum_{s,m}\sum_{i=1}^{t} f_i \log f_i\right] - \left[\sum_{s,m}(\sum_{i=1}^{t} f_i)\log(\sum_{i=1}^{t} f_i)\right] - \left[\sum_{i=1}^{t}(\sum_{s,m} f_i)\log(\sum_{s,m} f_i)\right] + \left[(\sum_{s,m}\sum_{i=1}^{t} f_i)\log(\sum_{s,m}\sum_{i=1}^{t} f_i)\right]\right), \quad (7)$$

where s and m are the two sample histograms, t is the total number of bins and f_i is the probability at bin i.

Then the similarity between two regions i and j is measured by the weighted sum of the similarity measures of spectral and texture distributions G_s and G_t,

考虑点之一：权重选择

$$W_G(i,j) = w_t G_t + w_s G_s \tag{8}$$

Because different regions have different attributes, the weights of texture and spectral distributions w_t and w_s should be adaptively determined in terms of different attributes of neighbouring regions. If both regions are smooth, the weight of spectral distribution should be large. If both regions have obvious texture characteristics, the weight of texture should be larger than that of spectral. The standard deviation (SD) can evaluate the smoothness of a region to a certain extent. A spectrally smooth image region results in a small SD and a spectrally rough image region results in a large SD. Thus, we use SD to evaluate the feature weights between two regions i and j.

We choose some smooth regions, like regions of water and grass, and compute their SDs that are less than 40 in most cases. So we regard a region with a SD less than 40 as a smooth region. If the SDs of neighbouring regions are both less than 40, we have:

$$\begin{aligned} u_s &= \max(S_i, S_j) \\ u_t &= \min(S_i, S_j). \end{aligned} \tag{9}$$

If the SD of a region is greater than the threshold, the equations for u_s and u_t become:

$$\begin{aligned} u_s &= \min(S_i, S_j) \\ u_t &= \max(S_i, S_j), \end{aligned} \tag{10}$$

where u_t and u_s are the weight estimations of the texture and spectral distributions respectively; S_i and S_j are the SDs of neighbouring regions i and j. We have the final result based on equation (8) after normalizing the weights,

$$\begin{aligned} w_t &= u_t/(u_t + u_s) \quad \text{高于40} \\ w_s &= u_s/(u_t + u_s), \quad \text{低于40} \end{aligned} \tag{11}$$

3. Segmentation methodology

The whole segmentation framework includes three steps: hierarchical splitting, modified agglomerative merging and pixel-wise refinement (see figure 4) similar to that used in Ojala and Pietikäinen (1999). In the hierarchical splitting step, the image is recursively split into four square sub-blocks of varying size based on a homogeneity measure:

$$R_h = \frac{W_{Gmax}}{W_{Gmin}} > X, \tag{12}$$

where W_{Gmax} and W_{Gmin} represent the largest and smallest homogeneities among the six pairwise homogeneities of the four sub-blocks. The initial maximum block size is set to 64 and the smallest block size is 16 to allow texture feature calculations. The blocks are recursively split into four sub-blocks when R_h is greater than a threshold X. The value of X depends on the spectral and texture characteristics of an image. X is experimentally set to 1.3 to 1.5 for regular texture images and 1.2 for H-res satellite imagery.

Once the image has been split into blocks of roughly uniform features, the blocks are merged through a modified merging procedure. At a particular stage of merging,

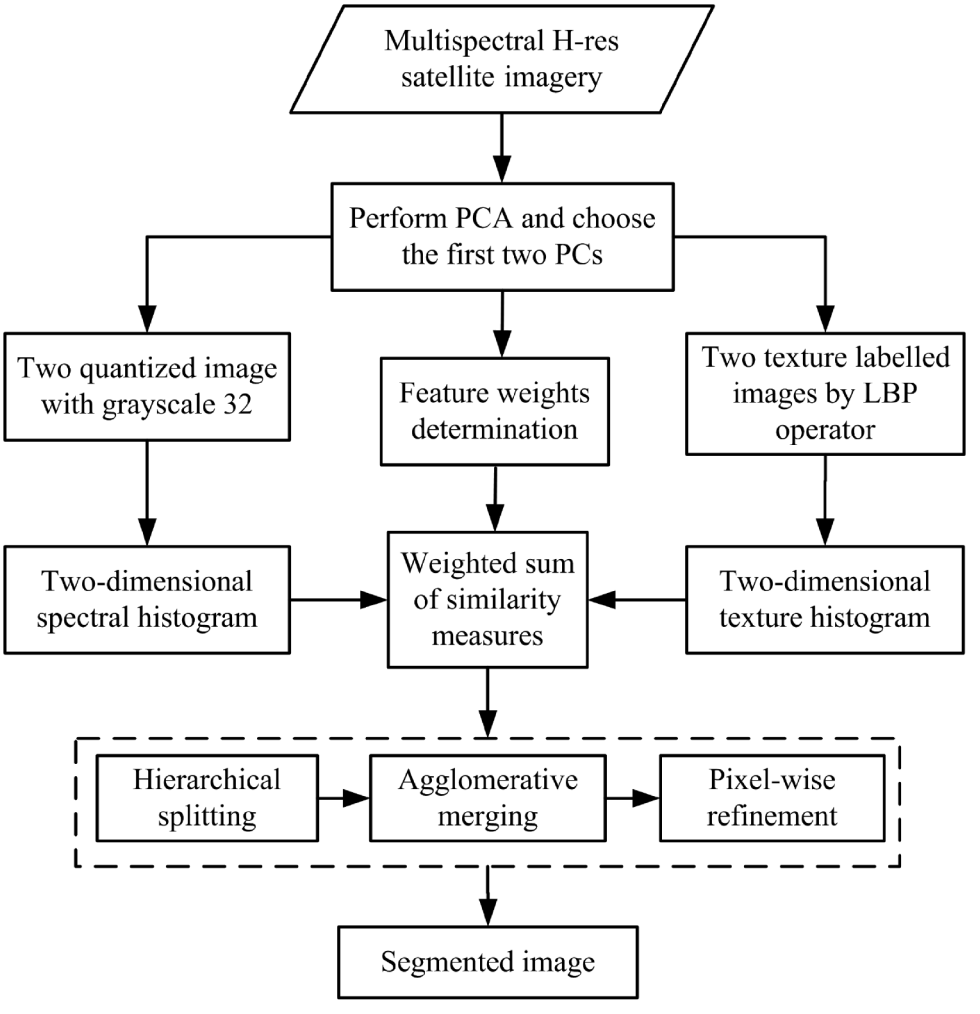

Figure 4. Region-based unsupervised segmentation by combining texture and spectral distributions.

等同于寻找最小合并代价

we merge that pair of adjacent regions which has the smallest merger importance (MI) value. MI is defined as:

$$M_I = \sqrt{p} \times W_G, \tag{13}$$

where p is the number of pixels in the smaller of the two regions and W_G is the weighted sum similarity measure between the two regions. The choice of M_I has some effect on the merging result. Although we can adopt $M_I = p \times W_G$ (Ojala and Pietikäinen 1999), it overrates the size of regions and makes the segmentation results unstable. In the merging process, we use a region adjacency graph (RAG) to describe the blocks after splitting. The RAG consists of three components: V, E and M. V is a set of region nodes recording the region labels. E is an adjacency matrix recording the pseudo-address of each region edge. The M matrix records the MI values of all the pairs of adjacent regions of an image. At each merging step, we search the smallest

MI value of the M matrix and merge the adjacent regions that have the smallest one. Then we adjust the RAG, and merge the pair of adjacent regions that has the smallest MI value in the changed M matrix. Merging proceeds until the following stopping criterion is true:

$$M_{IR} = \frac{M_{Icur}}{M_{I\max}} > Y, \tag{14}$$

where M_{Icur} and $M_{I\max}$ denote the MI for the current best merge and the largest MI of all preceding mergers. Threshold Y is determined experimentally by trial and error.

A boundary refinement algorithm is used to refine the boundaries of the blocky segmented image. For an examined boundary point P, we place a discrete square with a dimension d around the pixel and compute the MI between the square and the neighbouring regions of point P. The pixel is relabelled if the label of the neighbouring region that has the smallest MI value is different from the label of P. At the following step, we only consider the boundary points that were relabelled at the previous sweep. The procedure is iterative and proceeds until the number of the un-relabelled boundary pixels is less than 50 or the number of iterations is greater than 30.

4. Experiments and results

The objective of the present experiments was to evaluate the effectiveness of the novel features in segmentation of H-res remote sensing imagery. In addition, we investigated the effects of several parameters, i.e. LBP operators, weight determination, MI and thresholds, on segmentation results to optimize the SIMF algorithm. Furthermore, the approach was performed on colour mosaic texture images to demonstrate robustness of the segmentation method. As colour or multispectral images are most widely used and as these images can provide more information than greyscale images, our segmentation approach explicitly uses multispectral or colour information as part of the segmentation algorithm.

The performance of the method was evaluated with several 256 × 256 pixel multispectral IKONOS-2 and QuickBird satellite imageres (see figure 5 and 6) and colour textured mosaic images (see figure 7). IKONOS-2 and QuickBird data contain red, green, blue and near-infrared (NIR) channels with 4.0 m and 2.44 m spatial resolution respectively. The textured mosaic images were composed of texture images from the publicly available benchmark texture databases i.e. MIT Media Lab Vistex. They were also used by Chen and Chen (2002).

The original multispectral or colour images were transformed by PCA. We used the first two PCs for feature extraction. These two PCs represent more than 95% of the variance in the four original image bands. We computed texture images of the PCs by various LBP operators and got two LBP labelled images which were used to obtain the discrete two-dimensional texture histograms. The texture similarity of adjacent regions was calculated by the G-statistic. The spectral histograms were derived by the joint distribution of the greyscale pixel values of the PCs. The spectral similarity of adjacent regions was computed by the G-statistic from the spectral histograms. The first PC was used to calculate standard deviations of image regions which were used to determine the weights of the spectral and texture features. The weighted sum similarity measures were then applied to the whole segmentation process.

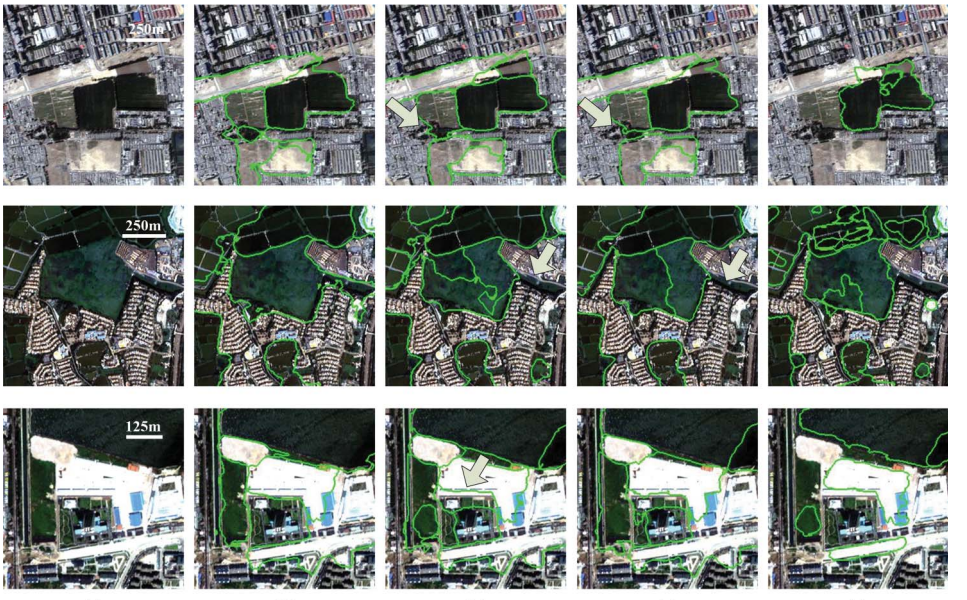

Figure 5. Segmentation with different weight combinations using texture distributions calculated by equation (5) where $P = 8$, $R = 1$ and spectral distributions. (*a*) Original images; (*b*) adaptive weight combination; (*c*) constant texture and spectral weights of 0.6 and 0.4; (*d*) using only spectral distributions; (*e*) using only texture distributions.

The experiments were conducted with different schemes, i.e. various LBP operators, different weight combinations, MI, thresholds and different kinds of colour images.

Figure 5 shows the segmentation results with different weight combinations. The LBP operator was $L_{8,1}^{ri}$. MI was calculated by equation (13), which yielded more robust and better results than $M_I = p \times W_G$ (Ojala and Pietikäinen 1999). The same splitting and merging thresholds were used for all H-res satellite images to demonstrate the robustness of the approach: $X = 1.2$ and $Y = 1.1$. In the process of boundary refinement, we placed a discrete square with dimension $d = 17$ around the boundary point P instead of a circle to reduce the complexity of computation. The segmentation results (see figure 5(*d*)) show that spectral distributions alone could not discriminate some regions. For example, the grass and trees regions of different texture characteristics in the first row of figure 5(*d*) were incorrectly segmented. As shown in figure 5(*e*), texture distributions alone could only discriminate those regions that have distinct texture characteristics. Texture and spectral distributions integrated by constant weights ($w_t = 0.6, w_s = 0.4$) yielded better results (see figure 5(*c*)), but some regions were still incorrectly segmented. The results (see figure 5(*b*)) that used adaptively integrated features based on equations (9)–(11) were most satisfying.

Figure 6 shows the segmentation results by spectral distributions adaptively combined with texture distributions obtained by different LBP operators. The LBP operators included $L_{8,1}$ (figure 6(*b*)), $L_{8,1}^{riu2}$ (figure 6(*c*)) and $L_{24,3}^{riu2}$ (figure 6(*d*)). The feature weights and MI were calculated by equations (9)–(11) and (13) respectively, which yielded good results in figure 5(*b*). The same set of threshold values, i.e. X, Y, d,

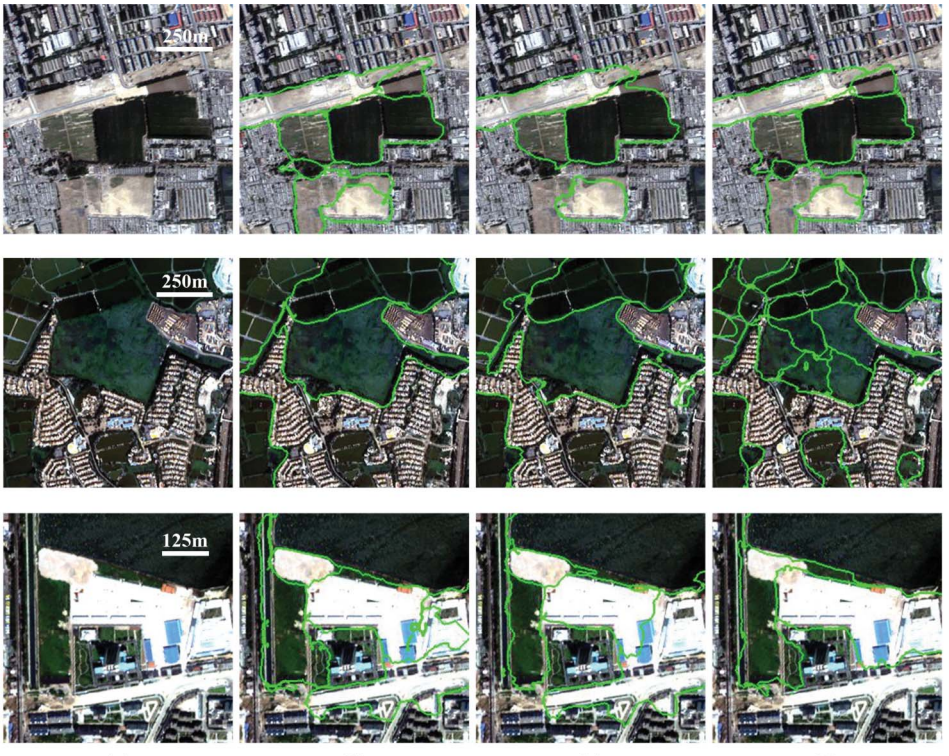

Figure 6. Segmentation with texture distributions calculated by different LBP operators and spectral distributions. (*a*) Original images; (*b*) using LBP operator in equation (1), where $P = 8$, $R = 1$; (*c*) and (*d*) using LBP operator in equation (3), where $P = 8$, $R = 1$ and $P = 24$, $R = 3$ respectively.

as that of figure 5 was used. As we can see from figure 6, the three LBP operators might perform well on some of the images but none of them was more stable than $L^{ri}_{8,1}$. A possible explanation for this is that the three LBP operators have their limitations when used on H-res satellite images. For example, $L_{8,1}$ is not rotation invariant, $L^{riu2}_{P,R}$ was proposed based on the 'Uniform' texture patterns of regular texture images, but most of the texture patterns of satellite images are non-uniform.

The performance of SIMF was further evaluated with several colour textured mosaic images. The parameter values were somewhat different from that applied to H-res satellite images: $X = 1.2$, $Y = 1.4$ and $d = 17$. The segmentation results (see figure 7(*c*)) of using only spectral distributions were good for some images (i.e. the top and bottom images). The results (see figure 7(*d*)) of using only texture distributions showed that most regions were not identified correctly except for the centre image. When the two features were integrated, the rough segmentation results (see figure 7(*a*)) were quite decent and the final segmentation results (see figure 7(*b*)) were excellent. The results demonstrate the robustness of the SIMF algorithm. The segmentation results by different LBP operators, including$L^{ri}_{8,1}$, $L_{8,1}$,$L^{riu2}_{8,1}$ and $L^{riu2}_{24,3}$, except $L^{riu2}_{24,3}$ which produced problem of boundary confusion, were fairly well since the colour texture images are simpler than H-res satellite imagery.

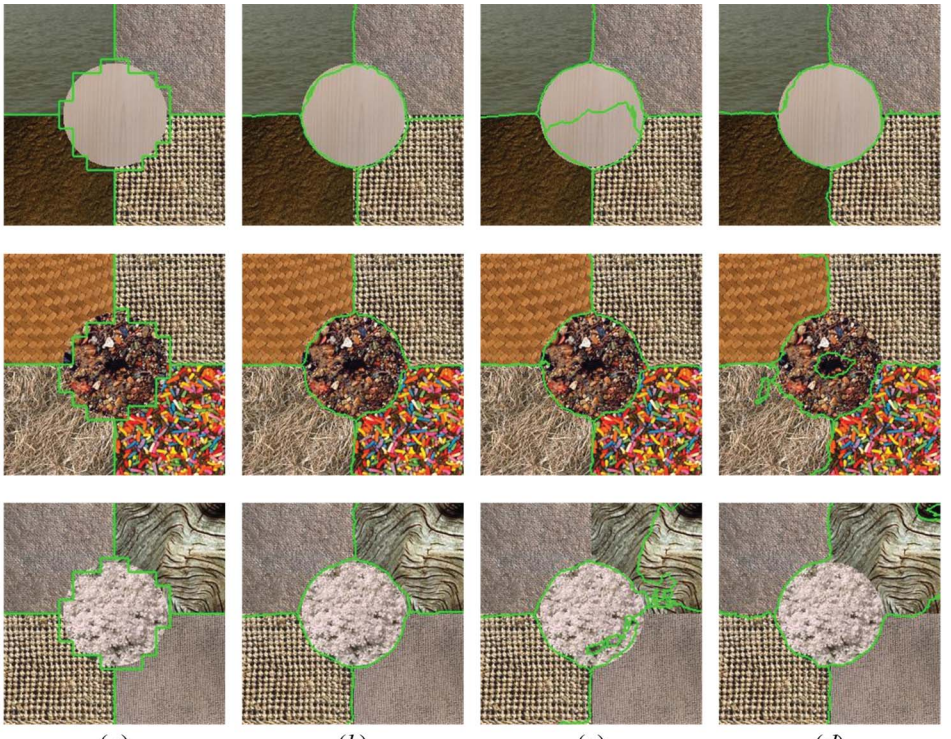

Figure 7. Segmentation of colour texture mosaics using texture distributions calculated by equation (5) where $P = 8$, $R = 1$ and spectral distributions. (*a*) Rough segmentation results by adaptive integrating texture and spectral distributions; (*b*) final results of (*a*); (*c*) using only spectral distributions; (*d*) using only texture distributions.

Figures 5, 6 and 7 demonstrate the effect of various parameters on the segmentation results by the SIMF approach. We generated satisfactory results (see figure 5(*b*)) based on adaptively integrated texture and spectral distributions for H-res satellite images. Figure 7(*b*) demonstrates the robustness of SIMF that yielding excellent performance on colour textured mosaic images.

5. Discussion and conclusion

This paper presented a novel feature extraction method that considers the cross-band relations between pixels and a new segmentation framework SIMF suitable for segmenting colour or multispectral images. Several experiments were carried out under different conditions: various LBP texture operators $L^{ri}_{8,1}$, $L_{8,1}$,$L^{riu2}_{8,1}$ and $L^{riu2}_{24,3}$, adaptive or constant weight combinations, different merger importance equations and two kinds of source images, to apply and evaluate the SIMF approach.

Although some LBP operators yield good segmentation results on some of the images, $L^{ri}_{8,1}$ was the most robust. Figure 5 illustrates the importance of applying a suitable weight choice for the spectral and texture features. The adaptive weight determination by standard deviation of regions is a novel aspect of this study. However, feature weight determination is still an important research topic for future

studies as most images are very complex. The segmentation approach performed comparatively well on simple colour texture mosaic images because of their simplicity.

Although we have generated some good segmentation results based on the feature extraction method in this study, the method has its limitations in image object discrimination. The first two PCs are on the directions of larger variance and contain most of the information of the original image, but there is no guarantee that the PCs contain appropriate and sufficient features for discrimination. Only when the new spectral values in the PCs coordinate system of two neighbouring objects are obviously different or they have very different texture features, the feature extraction method can be used to discriminate them easily.

The feature extraction method is very important for SIMF. Future research should concentrate on identifying more appropriate features that adapt to difference in image regions. The feature weight combination approach determines whether the combined features can discriminate heterogeneous regions to a large extent, which is still an open problem. M_I determines the sequence of merging of pairs of homogeneous regions. M_{IR} determines when to stop the merging process and the scale of segmentation results. Thus, future research should explore M_{IR} that can implement multiscale segmentation.

Acknowledgements

The authors would like to thank Dr Topi Mäenpää and Dr Xiangyun Hu for their valuable comments and discussions. The authors would also like to thank Ms Shu-yuan Chen for providing some of the image sources in this paper and the anonymous referees for their valuable comments.

References

Baatz, M. and Schäpe, A., 2000, Multiresolution segmentation: An optimization approach for high quality multi-scale image segmentation. In *Angewandte Geographische Informationsverarbeitung XII*, J. Strobl *et al*. (Eds), pp. 12–23 (Heidelberg: Wichmann).

Chen, K.-M. and Chen, S.-Y., 2002, Color texture segmentation using feature distributions. *Pattern Recognition Letters*, **23**, pp. 755–771.

Chen, Q.X., Zhou, C.H., Luo, J.C. and Ming, D.P., 2004. Fast segmentation of high-resolution satellite images using watershed transform combined with an efficient region merging approach. *Lecture Notes in Computer Science*, **3322**, pp. 621–630.

Chen, Z., Zhao, Z., Gong, P. and Zeng, B., 2006, A new process for the segmentation of high resolution remote sensing imagery. *International Journal of Remote Sensing*, **27**, pp. 4991–5001.

Gigandet, X., Cuadra, M.B., Pointet, A., Cammoun, L., Caloz, R. and Thiran, J.P., 2005, Region-based satellite image classification: method and validation. In *IEEE International Conference on Image Processing*, Genova, Italy, **3**, pp. III– 832–5.

Hay, G.J. and Castilla, G., 2006, Object-based image analysis: strengths, weaknesses, opportunities and threats (swot). Available online at: http://www.commission4.isprs.org/obia06/Papers/01_Opening%20Session/OBIA2006_Hay_Castilla.pdf (accessed 10 May 2007).

Hay, G.J., Blaschke, T., Marceau, D.J. and Bouchard, A., 2003, A comparison of three image-object methods for the multiscale analysis of landscape structure. *ISPRS Journal of Photogrammetry and Remote Sensing*, **57**, pp. 327–345.

Hay, G.J., Castilla, G., Wulder, M.A. and Ruiz, J.R. 2005, An automated object-based approach for the multiscale image segmentation of forest scenes. *International Journal of Applied Earth Observation and Geoinformation*, **7**, pp. 339–359.

Heikkila, M. and Pietikäinen, M., 2006, A texture-based method for modeling the background and detecting moving objects. *IEEE Transactions on Pattern Analysis and Machine Intelligence*, **28**, pp. 657–662.

Hu, X., Tao, C.V. and Prenzel, B., 2005, Automatic segmentation of high-resolution satellite imagery by integrating texture, intensity and color features. *Photogrammetric Engineering and Remote Sensing*, **71**, pp. 1399–1406.

Lucieer, A., Stein, A. and Fisher, P., 2005, Multivariate texture-based segmentation of remotely sensed imagery for extraction of objects and their uncertainty. *International Journal of Remote Sensing*, **26**, pp. 2917–2936.

Mäenpää, T., 2003, The local binary pattern approach to texture analysis-extensions and applications. Ph.D. Thesis, University of Oulu, Finland.

Ojala, T. and Pietikäinen, M., 1999, Unsupervised texture segmentation using feature distributions. *Pattern Recognition*, **32**, pp. 477–486.

Ojala, T., Pietikäinen, M. and Harwood, D., 1996, A comparative study of texture measures with classification based on feature distributions. *Pattern Recognition*, **29**, pp. 51–59.

Ojala, T., Pietikäinen, M. and Mäenpää, T., 2002, Multiresolution gray-scale and rotation invariant texture classification with local binary patterns. *IEEE Transactions on Pattern Analysis and Machine Intelligence*, **24**, pp. 971–987.

Ojala, T., Pietikäinen, M. and Mäenpää, T., 2006, A generalized local binary pattern operator for multiresolution gray scale and rotation invariant texture classification. Available online at: http://www.ee.oulu.fi/research/imag/texture (accessed 10 May 2007).

Pesaresi, M. and Benediktsson, J.A., 2001, A new approach for the morphological segmentation of high-resolution satellite imagery. *IEEE Transactions on Geoscience and Remote Sensing*, **39**, pp. 309–320.